Table 1 Comparison of estimated and actual lap times and velocities for 33 1983 qualifying vehicles

Disguised qualifier number	Official four lap time, s	Computed four lap time, s	Time based, % error	Official four lap speed, mph	Computed four lap speed, mph	Speed based, % error
Q1	188.292	184.798	−1.856	191.192	194.807	1.891
Q2	184.678	182.606	−1.122	194.934	197.146	1.135
Q3	180.014	178.156	−1.032	199.984	202.070	1.043
Q4	177.936	175.364	−1.445	202.320	205.287	1.467
Q5	178.635	175.261	−1.889	201.528	205.408	1.925
Q6	182.133	178.161	−2.181	197.658	202.064	2.229
Q7	183.008	180.396	−1.427	196.713	199.560	1.448
Q8	181.246	178.947	−1.268	198.625	201.177	1.285
Q9	180.400	176.857	−1.964	199.557	203.555	2.003
Q10	181.272	178.769	−1.381	198.597	201.377	1.400
Q11	199.976	194.797	−2.590	180.022	184.808	2.658
Q12	181.252	179.126	−1.173	198.618	200.976	1.187
Q13	196.565	193.686	−1.465	183.146	185.868	1.486
Q14	180.227	178.563	−0.923	199.748	201.609	0.932
Q15	181.601	179.474	−1.171	198.237	200.586	1.185
Q16	180.538	178.486	−1.137	199.404	201.696	1.150
Q17	178.213	175.615	−1.458	202.005	204.994	1.479
Q18	183.982	181.432	−1.386	195.671	198.421	1.406
Q19	182.179	180.795	−0.760	197.608	199.120	0.765
Q20	180.637	178.014	−1.452	199.295	202.231	1.473
Q21	184.513	181.720	−1.514	195.108	198.107	1.537
Q22	182.043	180.175	−1.026	197.755	199.806	1.037
Q23	180.096	177.886	−1.227	199.893	202.377	1.243
Q24	181.320	179.780	−0.849	198.544	200.244	0.856
Q25	179.903	177.670	−1.241	200.108	202.623	1.257
Q26	173.582	172.125	−0.839	207.395	209.150	0.846
Q27	176.742	174.874	−1.057	203.687	205.862	1.068
Q28	178.258	176.461	−1.008	201.954	204.011	1.018
Q29	176.211	174.253	−1.111	204.301	206.596	1.123
Q30	178.089	176.194	−1.064	202.146	204.320	1.075
Q31	186.535	183.120	−1.831	192.993	196.592	1.865
Q32	175.292	173.194	−1.197	205.372	207.859	1.211
Q33	183.729	181.505	−1.211	195.941	198.342	1.225

If $F_f = \mu x$ (the total normal force on the tires), then

$$F_c\cos\theta - \mu(F_a + F_w\cos\theta) - F_w\sin\theta = 0 \tag{4}$$

and the necessary downforce is then

$$F_a = \frac{(mv^2/r)\cos\theta - F_w\sin\theta - \mu F_w\cos\theta}{\mu} \tag{5}$$

where m is the vehicle mass. A coefficient of friction between tire and track of 1.6 is assumed. Changes in this coefficient will affect results.

The downforce requirements for each of the 33 1983 qualifiers are shown in Fig. 4 as a function of turn location. The downforce required in each of the long straightaways was assumed to be zero because no turning maneuver is being executed.

Conclusions

Downforce requirements for racing cars at IMS can be determined using the above techniques. Simulation results for both velocity and time show errors that are consistently in the 1-2% range, with many below 1%.

References

[1]Fisher, D.P., "Shortcomings of Radar Speed Measurements," *IEEE Spectrum*, Dec. 1980, pp. 28-31.

[2]"Computer Simulation of Watkins Glen Grand Prix Circuit Performance," Vehicle Research Department, Cornell Aeronautical Laboratory, Buffalo, N.Y., CAL Rept. ZL-500-K-1, New York, 1971.

[3]Technical Rules Bulletin, United States Auto Club, 4910 West 16th Street, Speedway, Indiana.

Slow and Fast State Variables for Three-Dimensional Flight Dynamics

M. Ardema*
NASA Ames Research Center
Moffett Field, California
and
N. Rajan†
Stanford University, Stanford, California

Introduction

BECAUSE of the complexity of the sixth-order point-mass equations of aircraft motion, there long has been interest in using reduced-order models in aircraft flight mechanics. This interest has increased greatly because of the development of singular perturbation methods for aircraft trajectory optimization.[1,2] The success of these methods depends essentially on identifying appropriate slow and fast state variables.

It is well known[2] that state variables altitude (h) and velocity (V) are approximately the same speed for supersonic aircraft and are, therefore, not time-scale-separable for

Received Oct. 4, 1984; revision received Dec. 6, 1984. This paper is declared a work of the U.S. Government and therefore is in the public domain.

*Research Scientist. Associate Fellow AIAA.

†Research Associate, Aeronautics and Astronautics Department. Member AIAA.

singular-perturbation analysis. Reference 3 presents a rational method of selecting suitable slow and fast variables. State variable transformations $\phi(h,V)$ and $\psi(h,V)$ are sought so that 1) ϕ is slow and ψ fast; 2) ϕ is independent of the (usually fast) flightpath angle γ; and 3) $\psi=0$ gives a value of γ consistent with the velocity-altitude profile of the reduced solution. It turns out, in the two-dimensional (vertical-plane) case considered in Ref. 3, that ϕ should be chosen as E (the specific excess energy); whereas, ψ should be chosen as $\partial P/\partial h\,|_E$, where P is the specific excess power. This choice for ψ gives a better estimate for γ along the reduced solution than either of the usual choices, $\psi=h$ or $\psi=V$. Thereby, the accuracy of singular-perturbation analyses is increased by decreasing the magnitude of boundary-layer corrections. In this note, we extend this approach for identifying slow and fast variables to the case of three-dimensional flight.

Analysis

The three-dimensional aircraft point-mass equations of motion are

$$\dot{x}=V\cos\gamma\sin\chi \tag{1}$$

$$\dot{y}=V\cos\gamma\cos\chi \tag{2}$$

$$\dot{h}=V\sin\gamma \tag{3}$$

$$\dot{V}=g(T-D-\sin\gamma) \tag{4}$$

$$\dot{\chi}=gL\sin\mu/V\cos\gamma \tag{5}$$

$$\dot{\gamma}=g(L\cos\mu-\cos\gamma)/V \tag{6}$$

where x and y are the horizontal positional coordinates; χ is the heading angle; γ is the flightpath angle; $T(h,V,\beta)$, $D(h,V,L)$, and L are the thrust, drag, and lift per unit weight, respectively; β is the throttle setting; and μ is the bank angle. Based on Ref. 2, it is assumed that x, y, and χ are slow state variables and that γ is fast. Following Ref. 3, we seek transformations $\phi(h,V)$ and $\psi(h,V)$ with the properties stated in the Introduction.

First to be considered here is ϕ. Differentiating it using Eqs. (3) and (4) gives,

$$\dot{\phi}=\phi_h\dot{h}+\phi_V\dot{V}=\phi_hV\sin\gamma+\phi_Vg(T-D-\sin\gamma) \tag{7}$$

where subscripts denote partial differentiation. To be independent of γ, we must have

$$\phi_hV-\phi_Vg=0 \tag{8}$$

This will be satisfied by

$$\phi(h,V)=h+(1/2g)V^2 \tag{9}$$

or by any once-differentiable function of this expression. Then

$$\dot{\phi}=\phi_Vg(T-D)=V(T-D)=P(h,V,L,\beta) \tag{10}$$

From Eq. (9), ϕ is just the specific energy, E, known to be a slow variable[2]; this is the same result obtained in Ref. 3.

For the determination of ψ in the three-dimensional case, a complication arises; one that is not present in the vertical-plane case. In the latter case, the reduced solution is uniquely defined by the energy-climb path. In the three-dimensonal case, however, there are many possible forms of the reduced solution and several of these are typically found in each trajectory.[4] For example, segments of the reduced solution may lie on a terrain limit, a maximum or minimum speed boundary, the corner velocity locus, or may be a local interior extremal. Since each segment is a path in the (h,V) plane, the path of the reduced solution at any point may be characterized by, say,

$$f(h,V)=0 \tag{11}$$

This gives

$$\frac{dV}{dh}=-\frac{f_h}{f_V} \tag{12}$$

But from Eqs. (3) and (4),

$$\frac{dV}{dh}=\frac{g(T-D-\sin\gamma)}{V\sin\gamma} \tag{13}$$

Solving this for $\sin\gamma$ and using Eq. (12),

$$\sin\gamma=\frac{T-D}{1-(V/g)(f_h/f_V)} \tag{14}$$

Differentiate ψ and using Eqs. (3) and (4) gives

$$\dot{\psi}=\psi_h\dot{h}+\psi_V\dot{V}=\psi_hV\sin\gamma+\psi_Vg(T-D-\sin\gamma) \tag{15}$$

Since ψ is to be fast, the right-hand side of Eq. (15) must vanish on the reduced solution giving

$$\sin\gamma=\frac{T-D}{1-(V/g)(\psi_h/\psi_V)} \tag{16}$$

In comparing Eqs. (14) and (16), we see that for the correct value of γ on the reduced solution

$$f_h/f_V=\psi_h/\psi_V \tag{17}$$

which will be satisfied by

$$\psi=f \tag{18}$$

or by any once-differentiable function of f.

The singularly perturbed version of the problem can now be stated as (changing notation from ϕ, ψ to E, f)

$$\dot{x}=V\cos\gamma\sin\chi \tag{19}$$

$$\dot{y}=V\cos\gamma\cos\chi \tag{20}$$

$$\dot{E}=P' \tag{21}$$

$$\dot{\chi}=gL\sin\mu/V\cos\gamma \tag{22}$$

$$\epsilon\dot{f}=f'_hV\sin\gamma+f'_Vg(P'-V\sin\gamma)/V \tag{23}$$

$$\epsilon\dot{\gamma}=g(L\cos\mu-\cos\gamma)/V \tag{24}$$

where $h(E,f)$ and $V(E,f)$ are to be determined from Eqs. (9) and (11), $P'(E,f,L,\beta)=P(h,V,L,\beta)$, $f'_h(E,f)=f_h(h,V)$, and $f'_V(E,f)=f_V(h,V)$. The reduced problem associated with Eqs. (19-24), however, is not the traditional energy-state dynamic model, unless the small γ assumption ($\sin\gamma=\gamma$, $\cos\gamma=1$) is made. If this assumption is made, the reduced problem is the energy-state model[4] regardless of whether h, V, or f is chosen as the fast variable ψ; this choice determines only the a posteriori calculation of γ.

We next determine the expressions for γ along the reduced solution for several specific cases (for small γ) that have been found to occur in practice.[4]

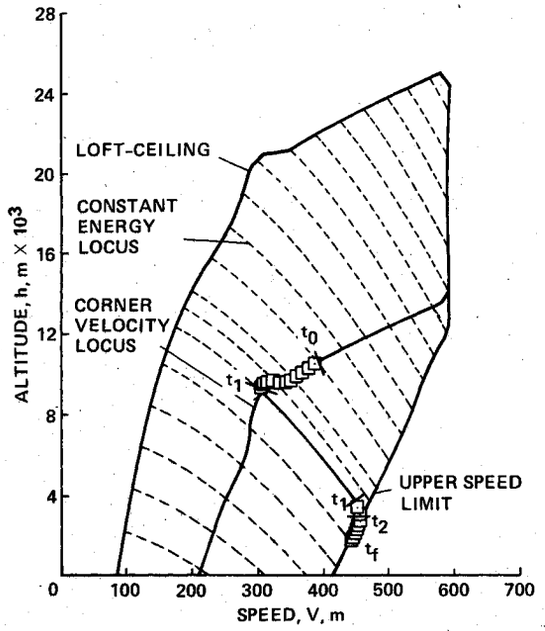

Fig. 1 Three-dimensional energy-state extremal.

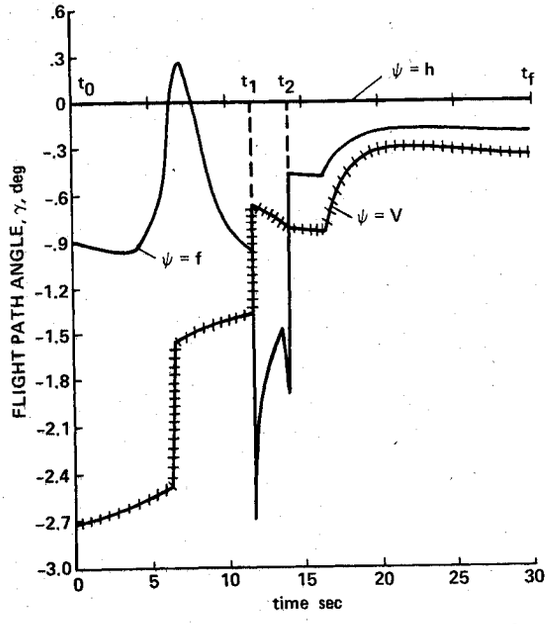

Fig. 2 Flightpath angle on energy-state extremal.

Special Cases

Terrain Limit

If the reduced solution is flight along a terrain limit, $h = h_T = \text{constant}$, then $f(h,V) = h - h_T = 0$ so that $f_h = 1$ and $f_V = 0$. From Eq. (14),

$$\gamma = 0 \tag{25}$$

on the reduced solution, as expected.

Velocity Bound

If the reduced solution is flight on a velocity bound, $V = V_M = \text{constant}$, then $f(h,V) = V - V_M = 0$ and

$$\gamma = T - D \tag{26}$$

Corner Velocity Locus

The corner velocity is defined as the velocity for which, at a given altitude, the maximum aerodynamic lift is equal to the structural maximum lift. Thus, on the reduced solution,

$$f(h,V) = C_{L_\alpha}(h,V)\alpha_M \rho(h) V^2 S - 2Wn = 0$$

where C_{L_α} is the lift curve slope; α_M, the maximum angle of attack; ρ, the atmospheric density; S, the wing reference area; W, the aircraft weight; and n, the maximum allowable load factor. This gives

$$f_h = 2Wn(C_{L_{\alpha_h}}/C_{L_\alpha}) + (\rho_h/\rho)$$

$$f_V = 2Wn(C_{L_{\alpha_V}}/C_{L_\alpha}) + (2/V)$$

and from Eq. (14),

$$\gamma = \frac{T - D}{1 - (V^2/g)[C_{L_{\alpha_h}} + (\rho_h C_{L_\alpha}/\rho)]/(VC_{L_{\alpha_V}} + 2C_{L_\alpha})} \tag{27}$$

Relative Local Minimum

Finally, suppose that the reduced solution is a relative local minimum. The calculation of γ by Eq. (14) is very tedious in this case, and it is easier to compute γ directly from

$$\gamma = \frac{T - D}{1 + (V/g)(\mathrm{d}V/\mathrm{d}h)} \tag{28}$$

where $\mathrm{d}V/\mathrm{d}h$ is determined numerically along the reduced solution.

Numerical Example

As an example, we choose an energy-state extremal from Ref. 4 (Fig. 1). The trajectory starts on the corner velocity (maximum instantaneous turn rate) locus at time t_0 and remains there until t_1. At t_1 the extremal jumps to a relative local minimum, and at t_2 the extremal intersects the Mach number constraint. It remains on this limit until termination at t_f.

Figure 2 shows the corresponding values of γ for the choices $\psi = h$, V, and f. The choice of $\psi = f$ generally gives a value of γ intermediate to the values given by $\psi = \mathrm{h}$ and $\psi = V$. The exceptions are the time intervals of approximately 6-8 s and 12-14 s. Here, in the first case, the sign in the slope of the corner velocity locus changes; and, in the second case, the extremal lies on the relative local minimum. The jump in the $\psi = V$ curve at 6 s is due to the throttle being switched from off to maximum, and the corners in the $\psi = f$ and $\psi = V$ curves at 16 s are due to the bank-angle control becoming unsaturated. Comparing the results shown in Fig. 2 with those of Ref. 3, the values of γ along the three-dimensional energy-state extremal are lower by approximately an order of magnitude than those along the two-dimensional energy-state solution. In fact, the values of γ in Fig. 2 are everywhere less than 3 deg, making the small γ assumption extremely good.

Concluding Remarks

A new fast variable for three-dimensional flight dynamics has been found. This variable has the advantage that it gives a value of flight-path angle consistent with the altitude and velocity state equations, thereby increasing the accuracy of the energy-state approximation and decreasing the magnitude of boundary-layer and higher-order corrections. In contrast to the two-dimensional case, the flight-path angles of the three-dimensional reduced-order extremals are quite small.

References

[1]Ardema, M.D., "An Introduction to Singular Perturbations in Nonlinear Optimal Control," *Singular Perturbations in Systems and Control,* CISM Courses and Lectures No. 280, edited by M.D. Ardema, International Centre for Mechanical Sciences, Udine, Italy, 1983, pp. 1-92.

[2]Ardema, M.D. and Rajan, N., "Separation of Time-Scales in Aircraft Trajectory Optimization," *Journal of Guidance, Control, and Dynamics*, Vol. 8, March-April 1985, pp. 275-278.
[4]Rajan, N. and Ardema, M.D., "Interception in Three-Dimensions: An Energy Formulation," *Journal of Guidance, Control, and Dynamics*, Vol. 8, Jan.-Feb. 1985, pp. 23-30.

An Analytical Approach to Geosynchronous Station Acquisition

Charles F. Gartrell*
General Research Corporation, McLean, Virginia

Introduction

GENERALLY, the effect of any transfer from low Earth orbit to geosynchronous orbit will be to place a spacecraft into an orbit located some distance away from the desired longitude or "station" with drift relative to that station. Consequently, a series of relatively small impulsive maneuvers must be performed to move the vehicle to the desired location and to eliminate the drift. A number of techniques and software systems have been devised to study this problem.[1,2] One common technique, such as that employed in the analysis program used for the SMS and GOES spacecraft, is to systematically examine all possible combinations of maneuvers satisfying a set of user-specified constraints.[3] These different "acquisition maneuver designs" can then be sorted to select one or more meeting some desired criteria. While such systems have proved useful, the alternative approach discussed here allows the analyst considerably more insight and control over the maneuver design process.

Optimized Station Acquisition Maneuver Design

Suppose that as a consequence of the transfer to geosynchronous orbit, the spacecraft is located at a longitude λ_0 with a drift rate of $\dot{\lambda}_0$, both of which are different from the desired station location λ_s and zero drift rate. There are two characteristics of the station acquisition scheme that must be established: the minimum velocity change necessary to produce the desired orbital characteristics and the order in which to apply the impulses to rotate the longitude to that desired orbit.

The minimum velocity change necessary to produce the proper orbital conditions can be found using a coplanar Hohmann transfer.[4] This velocity change (ΔV_T), while establishing the desired orbital altitude and shape, will not rotate the longitude from one location to another. In order to accomplish this, the velocity change is split a number of times to determine a series of intermediate orbits. These orbits are chosen such that

$$\Delta\lambda-\epsilon\le\sum_{i=0}^{N}R_i\dot{\lambda}_i\le\Delta\lambda+\epsilon \qquad (1)$$

where R_i is the number of days at each intermediate orbit i, $\dot{\lambda}_i$ the associated drift rate, $\Delta\lambda$ the longitude change desired, and ϵ a small tolerance about the desired station. Inspection of this result indicates that there seems to be no straightforward way of establishing an optimal set of impulsive burns.

Received July 9, 1984; revision received Nov. 30, 1984.

*Senior Engineer, Systems Technology Division—East. Member AIAA.

However, three basic constraints can put some limits upon the number of possible solutions. The first of these is a constraint on the maximum velocity change allowed for any one maneuver. This limit can be imposed by the nature of the spacecraft hardware (e.g., maximum thruster steady-state operation time) and avoidance of gravity losses incurred by excessively long maneuvers.[5] Another constraint is defined by the range of values allowed for the number of days in any of the intermediate orbits. The minimum value is nominally chosen to correspond to the least amount of time required to obtain adequate tracking data and to perform the processing necessary to determine the orbit of the satellite. This permits fine tuning of any subsequent maneuvers due to variations in thruster performance. The final constraint comes about by noting the ratio of required ΔV_T and the maximum ΔV allowed per maneuver. This value is the minimum number of burns needed to acquire station.

Having found the velocity change to effect the orbital transfer, a means is then necessary to estimate the minimum time to acquire the station. Noting that one part of the Hohmann transfer can initiate the drift to the station and that the second part can stop the drift once the station is reached, some coast time T between the two must be found. The desired drift rate to initiate the drift to station is simply $\Delta\lambda/T$. It can be noted that during the coast between maneuvers,

$$\lambda=\frac{1}{2}\left(\ddot{\lambda}_0+\frac{1}{2}\Delta\lambda\frac{\partial\ddot{\lambda}}{\partial\lambda_0}\right)t^2+\dot{\lambda}_0t+\lambda_0 \qquad (2)$$

This is a modification of the quadratic equations in Ref. 6 to reflect longitude variations greater than 1 deg. A key issue to this approach is the accuracy of this result. The direct numerical comparison of this equation and similar results from Ref. 7 for a 28 day epoch shows a 0.03 deg difference in longitude having started at the initial conditions of $\lambda=272.1$ deg and $\dot{\lambda}=-1.472$ deg/day. As can be observed, the differences are small. Thus, it can be concluded that this relation can be used with confidence.

The relation between velocity change and drift rate change [$\Delta V=|\Delta\dot{\lambda}/n|V_s/3|$] can now be exploited. The first velocity change can be related to the longitude difference by

$$\Delta V_1=\frac{V_s}{3n}\left[\frac{\Delta\lambda}{T}-\left(\ddot{\lambda}_0+\frac{1}{2}\Delta\lambda\frac{\partial\ddot{\lambda}}{\partial\lambda_0}\right)T-\dot{\lambda}_0\right]$$

and the second given as

$$\Delta V_2=\frac{V_s}{3n}\left[\frac{\Delta\lambda}{T}-\left(\ddot{\lambda}_0+\frac{1}{2}\Delta\lambda\frac{\partial\ddot{\lambda}}{\partial\lambda_0}\right)T\right]$$

Table 1 Example orbit and maneuver specifications

Specification	Initial orbit	Final orbit
Semi-major axis, km	42,279.2	42,165
Eccentricity	0.017	0.0002
Longitude, deg	272.1	230.0
Drift rate, deg/day	−1.472	0.0

$\Delta V_T=26.3$ m/s (Hohmann transfer), $\Delta V_{max}\approx 5$ m/s (pre maneuver)

Maneuver no.	ΔV m/s	Drift rate, deg/day
0	–	−1.472
1	−5.0	−3.233
2	−5.0	−4.994
3	−1.2	−5.417
4	5.03	−3.642
5	5.03	−1.867
6	5.04	−0.092